



In silico discovery and biophysical evaluation of novel 5-(2-hydroxybenzylidene) rhodanine inhibitors of DNA gyrase B

Matjaž Brvar^a, Andrej Perdih^a, Vesna Hodnik^b, Miha Renko^c, Gregor Anderluh^{b,d}, Roman Jerala^e, Tom Solmajer^{a,*}

^a National Institute of Chemistry, Laboratory for Biocomputing and Bioinformatics, Hajdrihova 19, 1001 Ljubljana, Slovenia

^b Biotechnical Faculty, Infrastructural Centre for Surface Plasmon Resonance, Večna pot 111, 1000 Ljubljana, Slovenia

^c Jozef Stefan Institute, Department of Biochemistry and Molecular Biology, Jamova 39, 1000 Ljubljana, Slovenia

^d National Institute of Chemistry, Laboratory for Biosynthesis and Biotransformation, Hajdrihova 19, 1001 Ljubljana, Slovenia

^e National Institute of Chemistry, Laboratory of Biotechnology, Hajdrihova 19, 1001 Ljubljana, Slovenia

ARTICLE INFO

Article history:

Received 3 November 2011

Revised 15 February 2012

Accepted 21 February 2012

Available online 3 March 2012

Keywords:

DNA gyrase enzyme

Virtual screening

Molecular docking

Antibacterial agents

Drug design

ABSTRACT

Bacterial DNA gyrase is an established and validated target for the development of novel antibacterials. In our previous work, we identified a novel series of bacterial gyrase inhibitors from the class of 4-(2,4-dihydroxyphenyl) thiazoles. Our ongoing effort was designated to search for synthetically more available compounds with possibility of hit to lead development. By using the virtual screening approach, new potential inhibitors were carefully selected from the focused chemical library and tested for biological activity. Herein we report on a novel class of 5-(2-hydroxybenzylidene) rhodanines as gyrase B inhibitors with activity in low micromolar range and moderate antibacterial activity. The binding of the two most active compounds to the enzyme target was further characterised using surface plasmon resonance (SPR) and differential scanning fluorimetry methods (DSF).

© 2012 Elsevier Ltd. All rights reserved.

1. Introduction

The occurrence of bacterial resistance to most known antibiotics is compelling scientists worldwide to discover new antibacterials directed to already known or recently discovered targets.¹ In the development of novel potential antibacterials with broad spectra of efficacy, scientists must take into account selective toxicity and satisfactory ADME properties.^{2,3} The progress in proteomics and genomics in recent years has accelerated the discovery of new potential targets suitable for the development of new drugs.^{4,5}

One of the most investigated and validated targets for antibacterials remains DNA gyrase, a unique bacterial type II topoisomerase belonging to the GHKL (gyrase, HSP 90, histidine kinase, MutL) enzyme family.^{6–9} The main role of DNA gyrase is the introduction of negative supercoils into a circular bacterial DNA molecule with concurrent ATP hydrolysis, while the DNA relaxation process is ATP independent. DNA gyrase bears a heterodimeric structure A2B2. The principal role of subunit A (GyrA) is the breakage and reunion of the double DNA strand, while subunit B (GyrB) is responsible for the ATP hydrolysis supplying sufficient amount of energy for the introduction of negative supercoils.^{7,8}

The only class of DNA gyrase inhibitors currently used in clinical practice are the 6-fluoroquinolones, which act by binding to the Gyrase A complex with double DNA strands preventing the reunion of both DNA strands.¹⁰ They are mostly used for the treatment of respiratory and urinary infections. However, due to some serious side effects, their clinical use is limited and new research in this field is necessary.^{11,12}

DNA gyrase is one of the enzymes susceptible to control of activity by the possibility of inhibition of ATP binding. The first natural GyrB inhibitors originating from the class of coumarins from the *Streptomyces* species were discovered in the 1950s.¹³ Novobiocin (**1**) with the IC₅₀ of 3 nM was licensed for clinical use but was quickly withdrawn from the market due to severe toxicity issues. Structurally related and even more potent chlorobiocin (CBN) has never been used in clinics. Nevertheless, several analogues possessing even higher inhibitory activity and lower toxicity have been synthesised.¹⁴

Clyothialidines represent a second class of natural GyrB inhibitors (**2**). They comprise a 12-membered lactone ring with an integrated pentapeptide chain attached to the resorcinol moiety.^{15–17} Despite their better potency and selectivity against homologous eukaryotic topoisomerases as novobiocin, they possess poor antibacterial activity in vivo due to high lipophilicity. Recently, several attempts to increase their water solubility and retain efficiency

* Corresponding author.

E-mail address: tom.solmajer@ki.si (T. Solmajer).

have been made.^{18–20} However, the bacterial cell membrane and outer membrane permeability remain important challenges to overcome. The inhibitory mechanism of both groups of natural inhibitors that act as competitive inhibitors of the ATP binding site has been extensively characterised using radiolabeled ligands and X-ray structural analysis.^{21,22}

In addition to cyclothialidine, natural flavonoids were also discovered to be potent DNA gyrase B inhibitors.²³ The moiety crucial for inhibition was shown to be a resorcinol ring as a part of a 3,5,7-trihydroxy-4*H*-cromen-4-one heterocycle, and the binding mode was characterised by various physicochemical techniques.²⁴

In recent years, the majority of research efforts, both in the industry and academia, directed towards the inhibition of the DNA gyrase B have been focused on the synthesis and structure-based fragment design of low molecular weight ligands. Based on the available X-ray structure, a hydrogen bond donor–acceptor pattern crucial for interactions with Asp73 and Thr165 residues and conserved water molecule was proposed as a favourable feature of gyrase inhibitors.²⁵ (Fig. 2).

The idea of the donor–acceptor pattern has been already incorporated into the design of heterocyclic rings such as pyrazoles^{26,27} and indazoles²⁸ where the strategy of the fragment based drug design has been proven to be extremely successful. The most potent compound had substantially higher inhibitory activity than novobiocin; however, it lacked in vivo activity due to high *logP* values. Furthermore, this interaction pattern was also confirmed when extended to partially exocyclic structures, as in indolinones,²⁹ triazines,³⁰ pyrimidines,³¹ benzimidazole ureas³² and Schiff bases of indoline-2,3-dione.³³ Phenols³⁴ and resorcinols,³⁵ which were discussed in our previous work, are further examples in which the incorporation of this pattern was successful. Several of the above-mentioned inhibitors have been determined to possess higher inhibitory activity than their natural precursors. However, only few of them have been introduced to the clinical trials thus far and none have progressed to clinical use yet.

The main objective of our present study was to identify low molecular weight inhibitors of the DNA gyrase enzyme (**4**) by utilising its structural similarity to the previously discovered 2,4-dihydroxyphenylthiazoles (**3**). By combining computational and experimental approaches, we first focused on the screening of large commercially available databases of compounds. We further developed the pharmacophore model based on the experimentally determined binding mode of the GR12222X compound (**2**) a nat-

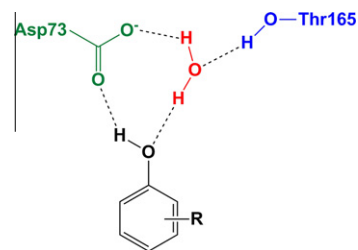


Figure 2. Hydrogen bond network formed between residues in the active site of GyrB and hydroxyl group of the phenol moiety.²⁵

ural cyclothialidine to G24, a 24 kDa N terminal fragment of GyrB, known to be the smallest fragment to still bind the ATP molecule. The phenol moiety was chosen as the starting fragment due to the conjecture (discussed above) that a single phenol hydroxyl group was shown to be sufficient for interaction of the first fragment with amino residues of the gyrase B active site.³⁴ In the search for the second fragment, the substituted thiazole ring was replaced by using a stepwise strategy of combining ligand-based and structure-based VS techniques, as presented in Figure 3. The inhibitory activity in vitro was determined for the compounds selected and purchased, and all active compounds were further characterised using surface plasmon resonance (SPR) and differential scanning fluorimetry (DSF) techniques. In addition, for active compounds, antibacterial activity on three different bacterial strains originating from *Staphylococcus aureus*, *Enterococcus faecalis* and *Haemophilus influenzae* was determined.

2. Results and discussion

2.1. Validation of docking and virtual screening tools

First we validated the ability of the GOLD docking software to reproduce the co-crystallised pose of the chlorobiocin within the ATP binding pocket of the G24 protein in the 1KZN crystal structure.³⁶ The best agreement between the docked and crystallised pose was achieved using the Goldscore scoring function (RMS of 0.55 Å, see Fig. S1 of Supplementary data). Based on the successful confirmation of reliability, this scoring function was used for the docking of the extracted base of the selected compounds.

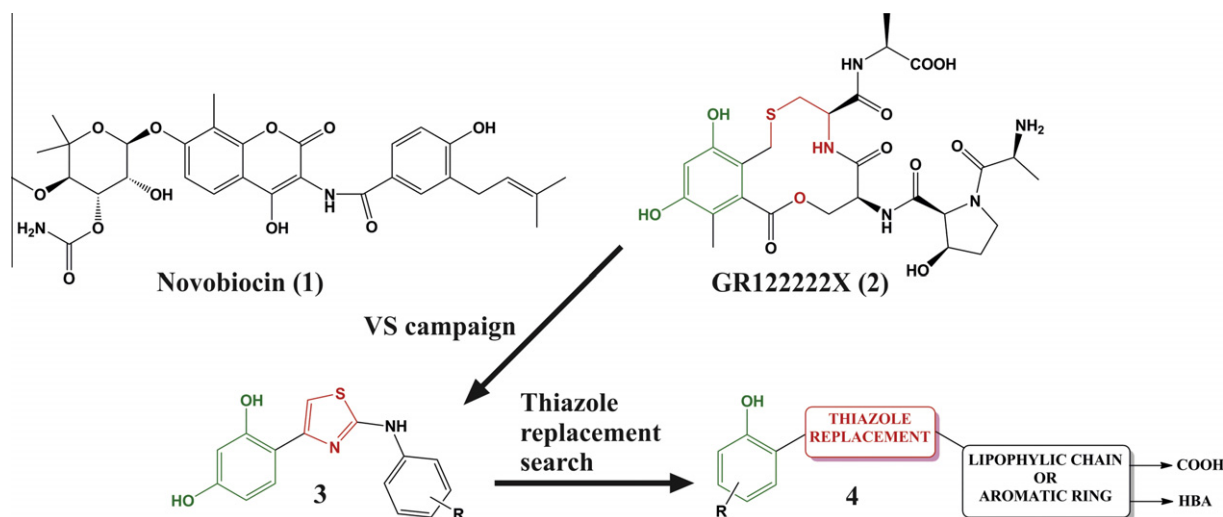


Figure 1. Chemical structures of novobiocin (**1**) and cyclothialidine (**2**). The structure of our previously reported inhibitor from the class of 2,4-dihydroxyphenylthiazoles (**3**)³⁵ and moieties that were optimised in this study (**4**).

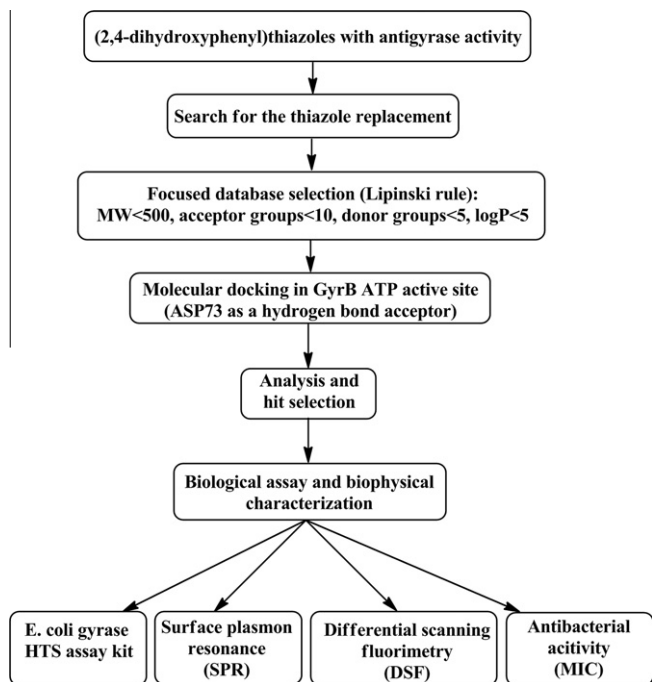


Figure 3. Design of the virtual screening campaign and subsequent biophysical characterisation of the hit compounds.

Since we utilised different docking software than in our previous study,³⁵ we additionally redocked a series of thiazole inhibitors in the G24 active site. Using similar constraints and the Goldscore scoring function, we successfully reproduced the docked poses of all five inhibitors from the previously reported structural class with, for example, RMS <0.49 Å for compound **9** of Ref. 35 (see Fig. S2 of Supplementary data for the comparison of both docked conformations for selected compounds from our previous study using structure-based pharmacophore model).

2.2. Thiazole replacement search

In the search for suitable thiazole replacements that would enable better optimisation of the hits, a new merged pharmacophore model was constructed based on the structure-based pharmacophores from our previous model yielding thiazole inhibitors.^{35,37} It was comprised of the hydrogen bond donor, hydrogen bond acceptor, negative ionisable group and three hydrophobic spheres. Exclusion volume spheres were added to model the spatial

restraints of the active site (See Fig. S3 of Supplementary data). Before proceeding to the next step of our VS campaign, the generated pharmacophore was validated for its ability to identify known hit compounds.³⁸ The pharmacophore model successfully identified all active compounds from the thiazole series.³⁵ These validation results provided confidence for the subsequent screening. (See Fig. S4 of Supplementary data).

Using LigandScout software, a virtual screening of a commercially available library of approximately five million compounds, all of which are converted into a multi-conformational format (see list of vendors in Supplementary data Section 2), returned approximately 4000 hits.³⁹

According to the position and pharmacophore fit score, compounds containing five different scaffolds (Fig. 3) were selected: rhodanines (2-sulfanylidene-1,3-thiazolidin-4-ones) (**5**), 1,3-thiazolidin-2,4-diones (**6**), 2-iminothiazolidin-4-ones (**7**), thiazolin-4-ones (**8**) and tiophenin-4-ones (**9**) (Fig. 5).

These scaffolds were selected according to the amount of commercially available compounds as well as the ability of hydrogen bond formation with the Asn46 residue. In addition, synthetic accessibility, an important consideration in drug design efforts, was also taken into account.⁴⁴ In addition, hit molecules from these classes were extracted from the e-molecules library.⁴⁰ 3-D structures of all hits were generated,⁴¹ and the focused library was docked into G24 ATP binding site using GOLD software.³⁶

2.3. Virtual screening of the selected compounds

Applying the Lipinski rule of five, we closely examined the focused library of approximately 1500 compounds containing selected scaffolds. This focused library extract was subsequently docked according to the criteria described in the Section 5. All calculated solutions were visually inspected and analysed for potential interactions with the amino acid residues, which are deemed to be important for binding (Fig. 6): hydrogen bonds with Asp73, Water 1001, Asn46 and hydrophobic interactions with Val43, Ile78, Ile90, Met91 and Val120 G24 residues.⁴² Values of the Gold Score scoring function were also examined, and 26 compounds were finally selected for purchase and subsequent biological evaluation.

2.4. In vitro screening of hit compounds for inhibitory activity

The enzyme assay for the determination of inhibitory activity was performed as described in Section 5.3. To eliminate the possibility of non-specific inhibition and to prevent aggregation, we used surfactants in all of our biological experiments.⁴³

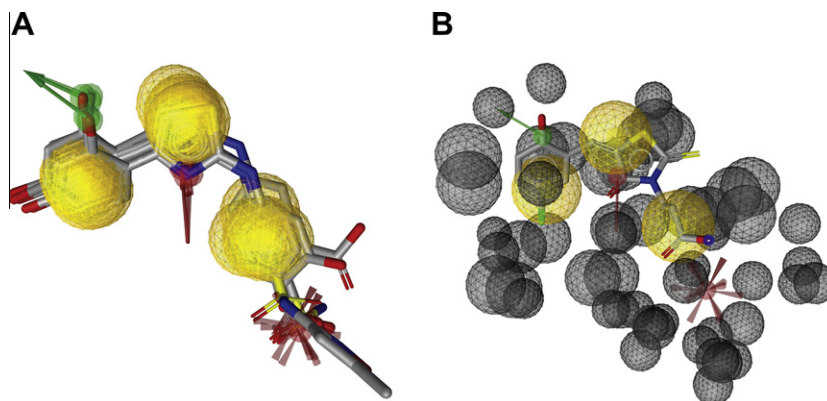


Figure 4. (A) Aligned docked 2,4-dihydroxyphenylthiazoles (compounds **5**–**9** of the Ref. 35) with pharmacophoric features displayed. The green arrow represents the hydrogen bond donor, the red arrow the hydrogen bond acceptor, a red sphere is a negative ionisable group and yellow spheres are hydrophobic pharmacophoric features. (B) Example of the GOLD-generated conformation of the virtual hit **14** aligned to the LigandScout pharmacophore.^{36,39} Exclusion volume spheres (grey spheres) represent the derived spatial restraints of the G24 protein ATP binding site.

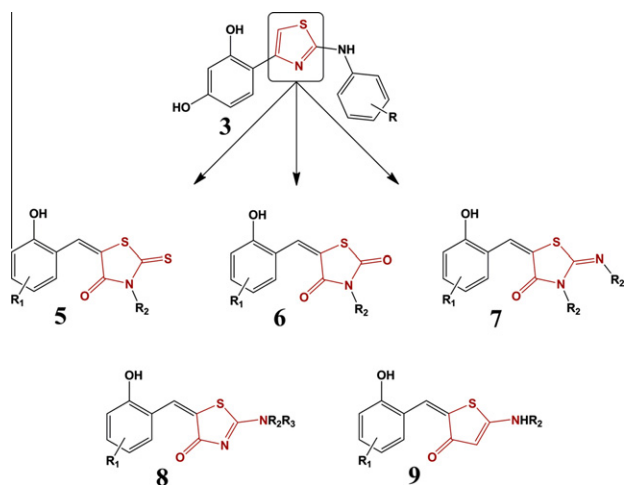


Figure 5. Five different heterocyclic scaffolds identified as suitable thiazole replacements.

The reaction was performed on streptavidin-coated black microtiter plates. Preliminary screening was performed at concentrations of 500, 125, 31.3 and 7.8 μM for each compound. All compounds showing some activity were further tested at 4 additional concentrations of 250, 62.5, 15.6 and 3.9 μM (8 all together) and IC_{50} was calculated using GraphPad Prism software. Obtained results are presented in Table 1.

2.5. Surface plasmon resonance (SPR) experiments

The SPR experiments were performed as described in the Section 5.5. After stabilisation of the baseline, the analytes were injected at 12 different concentrations and each titration was repeated three times. All sensorgrams showed immediate association between the protein and the analytes (Fig. 7) and responses were in good correlation with the increasing concentrations of the analytes. K_d values were calculated using the BiaEval software and results are shown in Table 1.

2.6. Differential scanning fluorimetry (DSF) experiments

Protein production, purification and DSF experiments were performed as described in Sections 5.4. and 5.6., respectively. Purified protein was subjected to a gradually (1 $^{\circ}\text{C}/\text{min}$) increasing temperature starting at 25 $^{\circ}\text{C}$. The temperature shift between the melting temperature (T_m) of the native protein and the protein–ligand complex is proportional to the stability of the latter. A bigger

temperature shift indicated higher stabilisation of a protein against thermal denaturation.

The experiments showed improvement in the protein stabilisation compared to the native G24 protein (Fig. 8). The best results were obtained using a complex of the G24 and compound **14** and the shift in T_m was 2.39 $^{\circ}\text{C}$. This observation substantiates the formation of the complex between the G24 protein and compound **14**, and the stabilisation of the protein upon the ligand binding.

2.7. Antibacterial activity

Active compounds **11–14** were tested against three bacterial strains: ATCC 29213 from *S. aureus*, ATCC 29212 from *E. faecalis* and ATCC 49766 from *H. influenzae* using the protocol as described in Section 5.7. Cefuroxime and gentamicin were included as reference compounds. The results of the antibacterial testing are presented in the Table 2. All tested compounds displayed some moderate antibacterial activity; among them, the bacterial strain ATCC 49766 from *H. influenzae* has shown the most sensitivity.

3. Discussion

In our efforts to discover novel compounds possessing antigrase activity, we tried to identify a novel class of synthetically easily available compounds that would allow fast and inexpensive hits to lead optimisation using the scaffold-hopping technique. We chose phenol moiety as a starting structural fragment for each compound as phenol inhibitors have already been reported in the literature and been shown to possess promising antigrase activity.³⁴ Based on our previous work in which we described a novel class of 2-amino-4-(2,4-dihydroxyphenyl) thiazoles (**3**) as gyrase B inhibitors, which were discovered starting from the structural data of the natural cyclothialidine inhibitors from *Streptomyces*,^{35,42} we have further examined the chemical space of possible thiazole replacements (Fig. 1) that would retain both the molecular recognition pattern features of initially discovered molecules on and intrinsically possess higher synthetic availability compared to the previous series.

Using a pharmacophore model, we discovered a novel class of GyrB inhibitors with promising inhibitory activity. In this study, aimed at synthetically easily available compounds we chose five different heterocyclic scaffolds: four partially or completely saturated thiazole analogues (**5–8**) and a partially saturated thiophene (**9**). From the database of commercially available compounds, we extracted and selected around 1500 compounds possessing a 2-hydroxybenzylidene moiety attached to the one of above

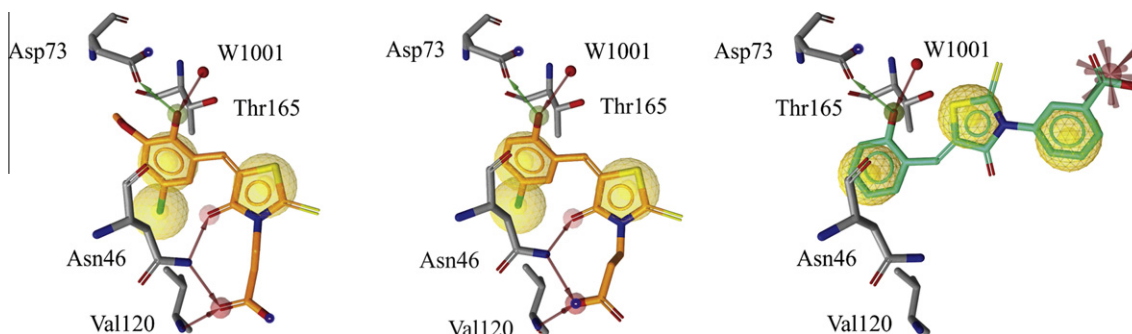
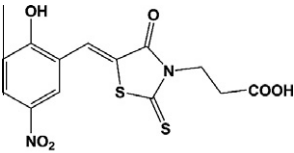
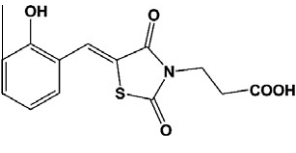
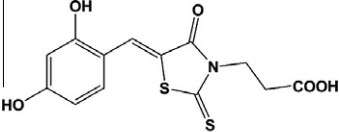
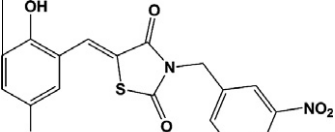
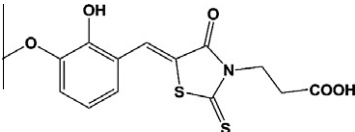
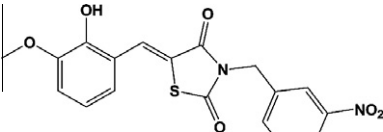
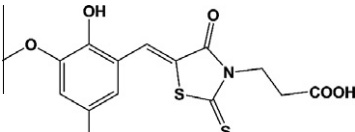
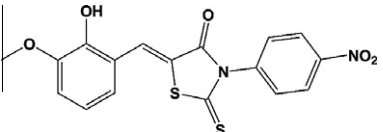
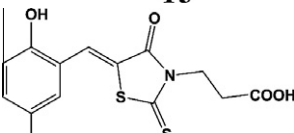
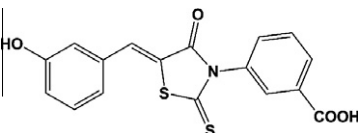
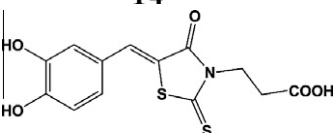
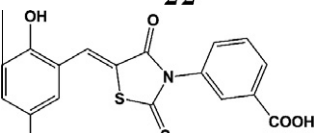
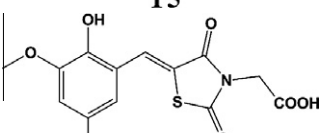
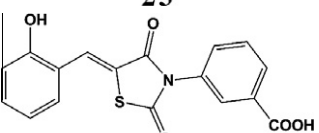
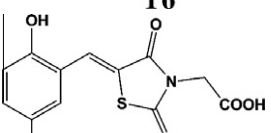


Figure 6. GOLD-calculated binding modes of the VS hit compounds **13** (left), **14** (middle) and **24** (right) docked into the G24 ATP binding site. Amino acid residues important for hydrogen bond formation are shown in grey (carbon atoms) and residues important for hydrophobic interactions (yellow spheres) are excluded due to greater transparency. Actives are shown in orange and inactive compounds in green.

Table 1
Selected compounds with inhibitory activity against the DNA gyrase and K_d values as determined by SPR experiments^a

Chemical structure	IC ₅₀ (μM)	K _d (μM)	Chemical structure	IC ₅₀ (μM)	K _d (μM)
	>1000	ND		>1000	ND
10			18		
	204	ND*		>1000	ND
11			19		
	680	ND*		>1000	ND
12			20		
	70	104±8		>1000	ND
13			21		
	64	62±17		>1000	ND
14			22		
	>1000	ND		>1000	ND
15			23		
	>1000	ND		>1000	ND
16			24		
	>1000	ND			
17					

ND—not detected due to the inactivity of a compound.

ND*—insufficient solubility at concentrations higher than 125 μM.

^a IC₅₀ of 0.015 μM was measured for novobiocin; as the reference standard (compared to 0.003 μM of Ref. 35).

mentioned heterocycles and performed a virtual screening campaign using GOLD software.³⁶

All poses were visually inspected and analysed for crucial interactions within the ATP binding site; 26 compounds with favourable Gold Score values, belonging to five different structural

classes (Fig. 5) were purchased and assayed for biological activity using a Gyrase *E. coli* enzyme assay kit (Inspiralis) and novobiocin acting as a reference standard (Table 1).⁴⁵ Only compounds from the class of rhodanines (5) were found to be active and are presented in Table 1 together with a class of thiazolidin-2,4-diones

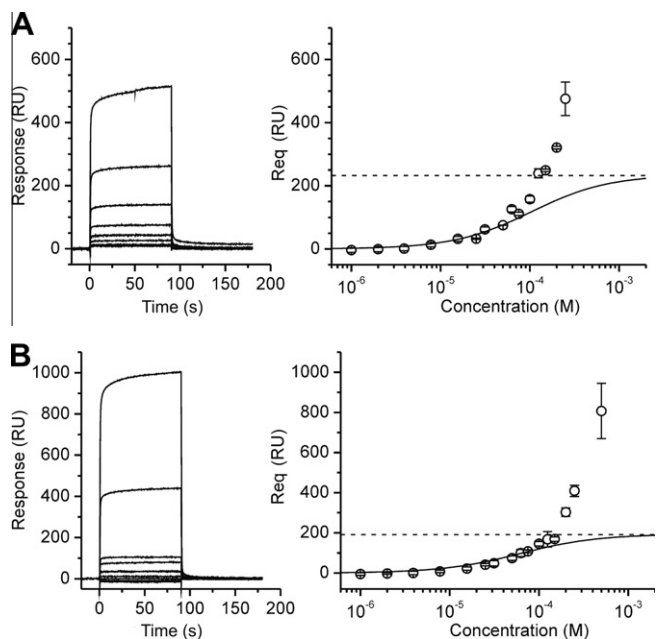


Figure 7. Sensorgrams (left) and experimental data fitted to the 1:1 binding model (right) for two most active compounds **13** (A) and **14** (B).

for easier comparison of the structural elements crucial for biological activity (the results of in vitro testing for all compounds **10–35** are available in [Supplementary data Table S1](#)).

Compounds **10–17** are rhodanines, N-substituted with the acetic or propionic acid, whereas compound **18** is a N-substituted thiazolidine-2,4-dione. Compound **19** and **20** bear a 3-nitrobenzyl substituent on the thiazolidine-2,4-dione ring, and compounds **21** to **25** are 4-nitrophenyl (**21**) or 3-carboxyphenyl (**22–25**) rhodanines. The range of antigrase activity of the active compounds **11–14** is still lower compared to the initial GR12222X cyclothialidone (**2**), a large cyclic molecule. This can be attributed to the fact that the discovered series of small molecules have considerably fewer available interactive sites for the interaction with the enzyme. However, the substitution possibilities of the identified inhibitors represent a good starting point for the further optimisation of these compounds.⁴⁴

Based on the seminal work of Luebbers et al.³⁴ we experimentally evaluated a change from resorcinols to differentially substituted phenols and in our limited SAR model we discovered that one hydroxyl group (at position 2 on phenyl ring) is enough for

Table 2
Antibacterial activity of tested compounds in $\mu\text{g}/\text{mL}$

Compound	<i>S. aureus</i> ATCC 29213	<i>E. faecalis</i> ATCC 29212	<i>H. influenzae</i> ATCC 49766
11	64	128	64
12	256	256	32
13	256	256	128
14	128	64	32
Cefuroxime	—	—	0.5
Gentamicin	0.5	8	—

the gyrase inhibition, and that substitution at position 4 is preferred over 2 or 3 substitution. Moreover, we discovered that the group on position 4 should be lipophilic rather than polarised (compound **10** having the 4-nitro substitution was found to be inactive).

The importance of a lipophilic group at position 4 is nicely shown in the case of compounds **12** and **13**, where the first one shows weak inhibition that is strengthened by the addition of the lipophilic group by a factor of 10. Furthermore, we noticed that an aliphatic chain is a better choice for the N-substitution on the rhodanine moiety than the phenyl ring. The length of the aliphatic chain was also shown to be of high importance, and while compounds **16** and **17** were found to be completely inactive, their homo analogues **13** and **14** had a K_d of 104 ± 8 and $62 \pm 17 \mu\text{M}$ respectively.

A comparison of compounds **11** and **15** clearly shows the importance of 2-hydroxyl group. While the compound **11** has IC_{50} of $204 \mu\text{M}$ the compound **15** has no activity against DNA gyrase.

Inspection of the docking results offers further insights to the experimental model observations. The binding modes of the two most active compounds **13** and **14** and inactive compound **24** are represented in [Figure 6](#). The hydroxylic group forms direct hydrogen bond with Asp73 and a water-mediated hydrogen bond with Thr165. The phenyl ring is seated in hydrophobic pocket and together with the lipophilic group at position 4 forms hydrophobic interactions with Val43, Ala47, Ile78, Met91, Val120 and Val167 residues (not all displayed in [Fig. 6](#) due to better visibility). The rhodanine ring was not only found to be an appropriate linker between the phenol ring and aliphatic chain, but is also capable of the hydrogen bond formation with Asn46 residue and hydrophobic interactions with Ile78 and Ile90 residues. Carboxylic group forms two hydrogen bonds with Asn46 and residue and amide proton of Val120 and it substantially contributes to the good water solubility of compounds. In contrast, compound **24** interacts only with Asp73. The absence of interactions with Asn46 and Val120 is, according to our model, responsible for the lack of inhibitory

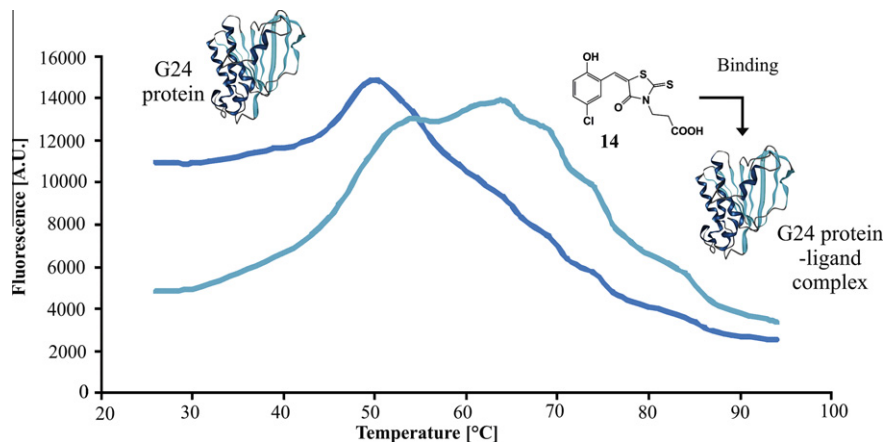


Figure 8. DSF experiment for compound **14** showing difference in thermal stability between the native G24 protein (dark blue) and G24 protein–compound **14** complex (cyan).

activity.³⁵ Additional hydrophobic interactions obviously do not contribute enough to improve the binding; neither does the carboxylic group, as it is moved far from the proposed position to interact with the Val120 residue.

The SPR experiments (Fig. 7) showed fast and tight binding of actives **13** and **14** to the G24 protein. At lower concentrations, the experimental observations were in a good agreement with the theoretical pharmacological model; however, at higher concentrations some unspecific binding of the ligands to the protein was observed, since responses were higher as theoretical ones. Maximal theoretical responses were calculated according to the molecular masses of the G24 protein and the inhibitors, and were used for fitting with the 1:1 binding model (Fig. 7). The obtained K_d values were in a low micromolar range, 62 ± 17 and $104 \pm 8 \mu\text{M}$ for compounds **13** and **14**, respectively. This confirms the formation of the ligand–protein complex, which was also characterised using the DSF technique for compound **14** (Fig. 8).

4. Conclusions

By combining virtual screening techniques with biophysical experiments, we successfully identified and experimentally characterised novel inhibitors of bacterial DNA gyrase. The focused database of commercially available compounds was screened for binding in the ATP binding pocket of the G24 protein and the most promising compounds were purchased and assayed for their biological activity. Three compounds (**11**, **13** and **14**) were found to possess antigyrase activity in a low micromolar range and an additional compound (**12**) was found to be weak inhibitor. All of them belong to the chemical class of the rhodanines, which makes them a suitable, synthetically available⁴⁴ replacement for the thiazole ring in a series of our previously reported inhibitors.³⁵ Furthermore, by performing SPR experiments, we confirmed the binding of the two most potent compounds (**13** and **14**) to the G24 protein, and a SAR analysis coupled with molecular docking calculations pinpointed some possibilities for the further optimisation of the hit series to increase the inhibitory activity of selected compounds. In addition, DSF experiments displayed an improvement in the protein stabilisation compared to the native G24 protein. Active compounds **11–14** were found to possess some antibacterial activity when tested against selected bacterial strains from *S. aureus*, *E. faecalis* and *H. influenzae*. Admittedly, extensive work on the cyclothialidine series^{18,20} has selected several compounds with low antibacterial activity, but our initial optimisation efforts starting from the cyclothialidine molecular recognition pattern showed that encouraging results could be obtained by using structure-based design principles. These promising novel low-molecular-weight hits, which are in accordance with the Lipinski rule of five, thus comprise a synthetically readily accessible chemical class of DNA Gyrase B inhibitors suitable for subsequent optimisation steps aimed at providing compounds for much-needed antibacterial drug development.

5. Materials and methods

5.1. Thiazole replacement search

Pharmacophore modeling software LigandScout was used for the search of possible novel thiazole replacements.⁴⁶ Pharmacophore model was constructed using GOLD-generated binding modes of 5 different inhibitors from the class of 2,4-dihydroxyphenylthiazoles.³⁵ All docked conformations of these compounds and created corresponding structure-based pharmacophores were aligned (Fig. 4A) and a merged pharmacophore was created (Fig. S3B) which comprised of a hydrogen bond donor, hydrogen bond acceptor, neg-

ative ionic center and three hydrophobic spheres. Exclusion volume spheres were also included to account for the protein environment. Successful pharmacophore model validation was performed as described in Section 2.2. The model was then screened against library of approximately 5 million commercially available compounds all previously converted in multiconformational format (25 conformers for each compound in the database).

5.2. Virtual screening procedure

Obtained initial conformation of the CBN molecule in the G24 (PDB 1KZN) was extracted from its active site and subsequently docked using GOLD molecular docking package.³⁶ The ATP binding site of G24 protein structure was used to define the active site resulting in a 10 Å cavity around the CBN position. In addition, as in our previous study a docking constraint was added determining Asp73 as a hydrogen bond acceptor.³⁵ A conserved water molecule interacting with Asn73 and Thr165 residues and the docked ligand molecule was also included in the docking procedure due to its importance revealed by the structural studies²⁵ Afterwards, CBN molecule was docked 10 times into the binding site by applying the following parameters of the GOLD genetic algorithm (GA) (Population size = 100, Selection pressure = 1.1, No. of Operations = 100000, No. of Islands = 5, Niche Size = 2, Migrate = 10, Mutate = 95, Crossover = 95). Several available scoring functions, (GOLDScore, CHEMScore and ASP) were used as fitness functions.³⁶

The results of the docking calculations demonstrated that GoldScore scoring function, which is comprised of four components (protein–ligand hydrogen bond energy, protein–ligand van der Waals energy, ligand internal van der Waals energy and ligand torsional strain energy), yielded the best docking results validated by the experimentally determined mode of CBN binding in G24. (see Supplementary data Figure S2).

5.3. Determination of IC₅₀ values

The assay for the determination of inhibitory activity was performed on black streptavidin-coated 96-well microplates. First they were rehydrated using wash buffer (20 mM Tris–HCl (pH 7.6), 137 mM NaCl, 0.01% (w/v) BSA, 0.05% (v/v) Tween 20). Then the biotinylated oligonucleotide was immobilized onto the wells (5 min at room temperature) and the excess oligo was washed off using the same buffer. Enzyme assay was carried out in reaction volume of 30 μL using 1 μg relaxed pNO1 as the substrate and 1.5 U gyrase from *E. coli*. Tested compounds were added as 100× stock in DMSO and final concentration of DMSO was 1% respectively. Reactions were incubated at 37 °C for 30 min, and then TF buffer (50 mM NaOAc (pH 5.0), 50 mM NaCl, 50 mM MgCl₂) was added to the wells and incubated at room temperature for another 30 min to allow triplex formation. Any unbound plasmid was washed off with TF buffer and SYBR Gold (Invitrogen) in T10 buffer (10 mM Tris–HCl (pH 8) and 1 mM EDTA) was added and allowed to stain for 20 min. After mixing, fluorescence was read using Tecan fluorimeter (Ex: 485 nm and Em: 535 nm) and Magellan software. IC₅₀ values were determined by measuring residual activity at eight (500, 250, 125, 62.5, 31.3, 15.6, 7.8 and 3.9 μM respectively) different concentrations and represent the concentration of inhibitor where residual activity is 50%.

5.4. Protein expression and purification

E. coli bacteria were grown at 37 °C with shaking (160 rpm) in LB media containing 150 μg/mL ampicillin until the OD reached 0.5–0.7. The protein expression was induced with 0.4 mM IPTG. After the expression the cells were harvested by centrifugation

(5500 rpm, 4 °C, 10 min) and suspended in lysis buffer containing 0.1% deoxycholic acid. The mixture was further sonified (amplitude 40%, 1 s on, 2 s off for 3 min) and centrifuged (12000 rpm, 4 °C, 15 min). To the supernatant a 20% streptomycin sulfate was added to the final concentration of 4% to remove the DNA and the dispersion was removed by centrifugation (12000 rpm, 4 °C, 15 min). The supernatant containing G24 protein was loaded onto a sepharose-novobiocin column and the protein was purified using affinity chromatography. Each loaded fraction was washed with 50 mL of 20 mM Tris–HCl (pH 8.0), 0.5 M NaCl, 25 mL of 100 mM NaAc (pH 4.0), 0.5 M NaCl and again 50 mL of Tris–HCl buffer. Protein was eluted with 8 M urea in 20 mM Tris–HCl (pH 7.5). Dialysis was performed 4 times overnight against Tris buffer (50 mM Tris–HCl pH 7.5, 1 mM EDTA, 2 mM DTT) and dialyzed protein was concentrated (3000 rpm, 4 °C). Purity was checked using SDS–PAGE method and commercially available protein molecular weight marker and the amount of each fraction was 10 µg of protein. The purity of the protein was determined to be >95% for each fraction (see Supplementary data, Figure S5).

5.5. Surface plasmon resonance (SPR) experiments, chip preparation and determination of K_D values

The surface plasmon resonance experiments for the compounds **13** and **14** were performed on a BiacoreT100 using CM5 sensor chip (Biacore, GE Healthcare). The system was primed twice with running buffer (10 mM Hepes, 150 mM NaCl, 3 mM EDTA, 0.005% P20, pH 7.4). The protein was immobilized on the second flow cell of a sensor chip CM5 using standard amino coupling method. Briefly, the carboxymethylated dextran layer was activated with 7 minute pulse of EDC (1-ethyl-3-(3-dimethylaminopropyl)-carbodiimide and NHS (*N*-hydroxy succinimide) mixed 1:1.⁴⁷ Protein was diluted to the final concentration of 50 µg/mL in 10 mM sodium acetate (pH 4.5) and injected in two short pulses to reach the final immobilization level around 13,500 response units. Finally, the rest of the surface was deactivated with 7 minute injection of ethanolamine. The first flow cell was activated with EDC/NHS and deactivated with ethanolamine and served as a reference cell for subtraction of nonspecific binding. Analytes were prepared as DMSO 100× stock solutions and were diluted with running buffer prior to the injection. They were injected at a flow-rate of 30 µL/min for 90 s and dissociation was monitored for additional 120 s. As the dissociation of analytes from the ligand was rapid, no regeneration protocol was needed. For the titration of analytes the 1% of the DMSO was added to the running buffer in order to diminish the difference in refractive index between samples and running buffer.

Both actives were tested at at least 8 different concentrations (depending on their solubility) in 3 parallel titrations. Some of the concentrations were injected several times to check for the reproducibility of the binding. The sensorgrams (Fig. 7) were analyzed using BiaEval software (Biacore, GE Healthcare). The equilibrium binding responses were determined from the binding levels five seconds before the stop of the injection. K_D values were determined by the fitting of the data to 1:1 steady state binding model as described in results.

5.6. Differential scanning fluorimetry (DSF) experiments

The initial optimization revealed that the optimal conditions are 15 µL of protein (2 mg/mL), 5 µL of dye (SYPRO orange, 1:100) and 10 µL of buffer (50 mM Tris–HCl pH 7.4, 1 mM EDTA, 5 mM DTT). In inhibitor test, 3 µL of inhibitor in DMSO (0.5 mM) were added.

The solutions were mixed and centrifuged and stepwise heated from 25 to 95 °C (1 °C/min). The fluorescence which rises when the protein is denaturated and hydrophobic amino acid residues are exposed to the dye was measured three times every minute Data

was processed using DSF spreadsheet and T_m values were calculated by fitting to the Boltzmann equation using Grafit.⁴⁸ All the experiments were performed in three parallels and changes of T_m between the native protein and the complex were calculated. The results of the experiment are shown in the Figure 8.

5.7. Antibacterial activity

The antibacterial activity study was performed at the Department of Microbiological Surveillance and Research, Statens Serum Institute in Copenhagen, Denmark. Fresh overnight colonies from 5% horse blood agar plates or chocolate agar plates were suspended to a turbidity of 0.5 McFarland and further diluted 1:100 in MH or HTM broth. 1024 mg/mL stock solutions of tested compound were prepared in DMSO and stock solutions of standards (gentamicin, cefuroxime) were prepared in sterile water. All microtiter plates were added 50 µL of MH/DMSO (*S. aureus* and *E. faecalis*) or HTM/DMSO (*H. influenzae*). For control compounds, only broth without DMSO was added. 50 µL of relevant solutions were added to the first row and then diluted 1:1. A total of 50 µL diluted bacterial suspension was added to wells containing 50 µL of two-fold compound-dilutions. Test range was 256–0.25 µg/mL. The plates were incubated at 35 °C in ambient air for 16–20 h for *S. aureus* and *E. faecalis* and 20–24 h for *H. influenzae*. Colony counts of the used inoculum were correct i.e. 1×10^6 CFU/mL and all control compounds were within the limits according to CLSI. All experiments were performed in triplicate and the results, MIC in µg/mL, are shown in Table 2.

Acknowledgements

This work was supported by the Ministry of Higher Education, Science and Technology of the Republic of Slovenia (grant J1-308 to T.S., young researcher grant 1000-08-310063 to M.B. and post-doctoral grant Z1-4111 to A.P.). We are sincerely grateful to Mr. R. Bremsak (National Institute of Chemistry, Laboratory of biotechnology) for help with expression and purification of G24. The authors would like to thank Laboratory of Biomolecular Structure at the National Institute of Chemistry for sharing their laboratory capacities. Mr. Terry Jackson is thanked for critical reading of the manuscript.

A. Supplementary data

Supplementary data associated with this article can be found, in the online version, at doi:10.1016/j.bmc.2012.02.052. These data include MOL files and InChIKeys of the most important compounds described in this article.

References and notes

- Brown, E. D.; Wright, G. D. *Chem. Rev.* **2005**, *105*, 759.
- Silver, L. L. *Biochem. Pharm.* **2006**, *71*, 996.
- Perdih, A.; Kovac, A.; Wolber, G.; Gobec, S.; Solmajer, T. *Bioorg. Med. Chem. Lett.* **2009**, *19*, 2668.
- Smith, C. *Nature* **2004**, *428*, 225.
- Rajcevic, U.; Niclou, S. P.; Jimenez, C. R. *Front Biosci.* **2009**, *14*, 3292.
- Maxwell, A.; Lawson, D. M. *Curr. Top. Med. Chem.* **2003**, *3*, 283.
- Maxwell, A. *Trends Microbiol.* **1997**, *5*, 102.
- Champoux, J. J. *Annu. Rev. Biochem.* **2001**, *70*, 369.
- Collin, F.; Karkare, S.; Maxwell, A. *Appl. Microbiol. Biotechnol.* **2011**, *92*, 479.
- Hooper, D. C. *Lancet. Infect. Dis.* **1992**, *1995*, 345.
- Drlica, K.; Malik, M. *Curr. Top. Med. Chem.* **2003**, *3*, 249.
- Minovski, N.; Perdih, A.; Solmajer, T. *J. Mol. Model.* **2011**. doi:10.1007/s00894-011-1179-0.
- Gilbert, E. J.; Maxwell, A. *Mol. Microbiol.* **1994**, *12*, 365.
- Musicki, B.; Periers, A. M.; Laurin, P.; Ferroud, D.; Benedetti, Y.; Lachaud, S.; Chatreaux, F.; Haesslein, J. L.; Iltis, A.; Pierre, C.; Khider, J.; Tessot, N.; Airault, M.; Demasse, J.; Dupuis-Hamelin, C.; Lassaigne, P.; Bonnefoy, A.; Vicat, P.; Klich, M. *Bioorg. Med. Chem. Lett.* **2000**, *10*, 1695.

15. Nakada, N.; Shimada, H.; Hirata, T.; Aoki, Y.; Kamiyama, T.; Watanabe, J.; Arisawa, M. *Antimicrob. Agents Chemother.* **1993**, *37*, 2656.
16. Nakada, N.; Gmuender, H.; Hirata, T.; Arisawa, M. *J. Biol. Chem.* **1995**, *270*, 14286.
17. Oram, M.; Dosanjh, B.; Gormley, N. A.; Smith, C. V.; Fisher, L. M.; Maxwell, A.; Duncan, K. *Antimicrob. Agents Chemother.* **1996**, *40*, 473.
18. Goetschi, E.; Anghern, P.; Gmuender, H.; Hebeisen, P.; Link, H.; Masciadri, R.; Nielsen, J. *Pharmac. Ther.* **1993**, *60*, 367.
19. Rudolph, J.; Theis, H.; Endermann, R.; Johannsen, L.; Geschke, F.-L. *J. Med. Chem.* **2001**, *44*, 619.
20. Anghern, P.; Buchmann, S.; Funk, C.; Goetschi, E.; Gmuender, H.; Hebeisen, P.; Kostrewa, D.; Link, H.; Luebbbers, T.; Masciadri, R.; Nielsen, J.; Reindl, P.; Ricklin, F.; Schmitt-Hoffmann, A.; Theil, F.-P. *J. Med. Chem.* **2004**, *47*, 1487.
21. Oblak, M.; Kotnik, M.; Solmajer, T. *Curr. Med. Chem.* **2007**, *14*, 2033.
22. Bradbury, B. J.; Pucci, M. J. *Curr. Opp. Pharm.* **2008**, *8*, 574.
23. Qushnie, T. P.; Lamb, A. J. *Int. J. Antimicrob. Agents.* **2005**, *26*, 343.
24. Plaper, A.; Golob, M.; Hafner, I.; Oblak, M.; Solmajer, T.; Jerala, R. *Biochem. Biophys. Res. Comm.* **2003**, *306*, 530.
25. Holdgate, G. A.; Tunnicliffe, A.; Ward, W. H. J.; Weston, S. A.; Rosenbrock, G.; Bart, P. T.; Taylor, I. W. F.; Pauptit, R. A.; Timms, D. *Biochemistry* **1997**, *36*, 9663.
26. Tanitame, A.; Oyamada, Y.; Ofuji, K.; Fujimoto, M.; Iwai, N.; Hiyama, Y.; Suzuki, K.; Ito, H.; Terauchi, H.; Kawasaki, M.; Nagai, K.; Wachi, M.; Yamagishi, J. *J. Med. Chem.* **2004**, *47*, 3693.
27. Ronkin, M. S.; Badia, M.; Bellon, S.; Grillot, A.-L.; Gross, C. H.; Mani, N.; Parsons, J. D.; Stamos, D.; Trudeau, M.; Wei, Y.; Charifson, P. S. *Bioorg. Med. Chem. Lett.* **2010**, *20*, 2828.
28. Boehm, H. J.; Boehringer, M.; Bur, D.; Gmuender, H.; Huber, W.; Klaus, W.; Kostrewa, D.; Kuehne, H.; Luebbbers, T.; Meunier-Keller, N.; Mueller, F. *J. Med. Chem.* **2000**, *43*, 2664.
29. Oblak, M.; Golic Grdadolnik, S.; Kotnik, M.; Jerala, R.; Filipic, M.; Solmajer, T. *Bioorg. Med. Chem. Lett.* **2005**, *15*, 2507.
30. Poyser, J. P.; Telford, B.; Timms, D.; Block, M. H.; Hales, N. J. WO 99/01442 1999.
31. Luebbbers, T.; Anghern, P.; Gmuender, H.; Herzig, S.; Kulhanek, J. *Bioorg. Med. Chem. Lett.* **2000**, *10*, 821.
32. Charifson, P. S.; Grillot, A. L.; Grossman, T. H.; Parsons, J. D.; Badia, M.; Bellon, S.; Deininger, D. D.; Drumm, J. E.; Gross, C. H.; LeTiran, A.; Liao, Y.; Mani, N.; Nicolau, D. P.; Perola, E.; Ronkin, S.; Shannon, D.; Swenson, L. L.; Tang, Q.; Tessier, P. R.; Tian, S.-K.; Trudeau, M.; Wang, T.; Wei, Y.; Zhang, H.; Stamos, D. *J. Med. Chem.* **2008**, *51*, 5243.
33. Aboul-Fadl, T.; Abdel-Aziz, H. A.; Abdel-Hamid, M. K.; Elsaman, T.; Thanassi, J. *Molecules* **2011**, *16*, 7864.
34. Luebbbers, T.; Anghern, P.; Gmuender, H.; Herzig, S. *Bioorg. Med. Chem. Lett.* **2007**, *17*, 4708.
35. Brvar, M.; Perdih, A.; Oblak, M.; Peterlin Masic, L.; Solmajer, T. *Bioorg. Med. Chem. Lett.* **2010**, *20*, 958.
36. Jones, G.; Willett, P.; Glen, R. C.; Leach, A. R.; Taylor, R. *J. Mol. Biol.* **1997**, *267*, 727.
37. Wolber, G.; Dornhofer, A.; Langer, T. *J. Comput. Aided Mol. Design* **2006**, *20*, 773.
38. Kirchmair, J.; Markt, P.; Distinto, S.; Wolber, G.; Langer, T. *J. Comput. Aided Mol. Design* **2008**, *22*, 213.
39. Wolber, G.; Langer, T. *J. Chem. Inf. Model.* **2005**, *45*, 160.
40. www.emolecules.com.
41. Wenlock, M. C.; Austin, R. P.; Barton, P.; Davis, A. M.; Leeson, P. D. *J. Med. Chem.* **2003**, *46*, 1250.
42. Lewis, R. J.; Singh, O. M.; Smith, C. V.; Skarzynski, T.; Maxwell, A.; Wonacott, A. J.; Wigley, D. B. *EMBO J.* **1996**, *15*, 1412.
43. Ryan, A. J.; Gray, N. M.; Lowe, P. N.; Chung, C. *J. Med. Chem.* **2003**, *46*, 3448.
44. Mendgen, T.; Steuer, C.; Klein, C. D. *J. Med. Chem.* **2012**, *55*, 743.
45. Maxwell, A.; Burton, N. P.; O'Hagan, N. *Nucl. Acids Res.* **2006**, *34*, e104.
46. Tomasic, T.; Peterlin-Masic, L. *Curr. Med. Chem.* **2009**, *16*, 1596.
47. de Mol, N. J.; Fischer, M. J. E.; Castrop, J.; Frelink, T. *Biomol. Interact.* **2006**, *18*, 19.
48. Niesen, F. H.; Berglund, H.; Vedadi, M. *Nature protoc.* **2007**, *2*, 2212.